ELSEVIER

Journal of Hydrology 223 (1999) 221–229

Journal of Hydrology

www.elsevier.com/locate/jhydrol

Modeling of earthquake-induced hydrological changes and possible permeability enhancement due to the 17 January 1995 Kobe Earthquake, Japan

T. Tokunaga

Department of Geosystem Engineering, University of Tokyo, 7-3-1 Hongo, Bunkyo-ku, Tokyo 113-8656, Japan

Received 12 November 1998; accepted 21 July 1999

Abstract

Hydrologic changes associated with the 17 January 1995 Kobe Earthquake occurred in Awajishima Island very close to the epicenter. These included: (1) large drop of water table in the mountainous area; (2) rapid increase of discharge along active faults; and (3) change of chemistry of discharged water. A simple horizontal flow model was constructed to explain the observed changes; and optimal sets of specific yield and the change of hydraulic conductivity were estimated. Results suggest that this model can explain the observed phenomena consistently. The hydraulic conductivity is estimated to increase at least five times than that before the Earthquake; however, quantitative measurement of the increase of discharge just after the earthquake would constrain better the change of the hydraulic conductivity. The specific yield of the unconfined aquifer is between 0.3 and 1.7% depending on the assumed recharge rate but independent of the assumed depth to the impermeable basement. The change in chemical composition of the discharged water could be explained by the upward movement of deeper water due to the invasion of saltwater into the aquifer. © 1999 Elsevier Science B.V. All rights reserved.

Keywords: Kobe earthquake; Hydraulic conductivity; Specific yield; Dupuit–Ghyben–Herzberg model

1. Introduction

Hydrologic changes occur in response to large earthquakes, and various mechanisms have been postulated to explain them (e.g. Sibson, 1981; Muir-Wood and King, 1993; Rojstaczer et al., 1995). It has been reported that similar hydrologic fluctuations were associated with the Hyogoken Nanbu (Kobe) Earthquake in Awajishima Island (Fig. 1) (Sato et al., 1995; Groundwater Research Group, Osaka City University Investigation Team for the HanshinAwaji Great Earthquake Disaster (hereafter called GRG), 1996; Oshima et al., 1996; Sato and Takahashi, 1996). These can be summarized as follows: (1) A large amount of water was discharged in the mountainous area just after the Earthquake, and this effect ended within 4 months (Oshima et al., 1996). (2) The water table in the central part started to drop soon after the Earthquake (Fig. 2; Table 1), and water levels of small ponds also started to drop and some of them dried up (GRG, 1996; Oshima et al., 1996; Osada et al., 1997). (3) On the contrary, the volume of discharged water near active faults increased rapidly and this anomalous discharge has continued for more than 1 year (Fig. 3) (Sato and Takahashi, 1996). (4) The chemical composition of discharged water has slightly increased in bicarbonate after the Earthquake (Fig. 4) (Sato et al., 1995;

E-mail address: tokunaga@geosys.t.u-tokyo.ac.jp (T. Tokunaga)

0022-1694/99/$ - see front matter © 1999 Elsevier Science B.V. All rights reserved.
PII: S0022-1694(99)00124-9

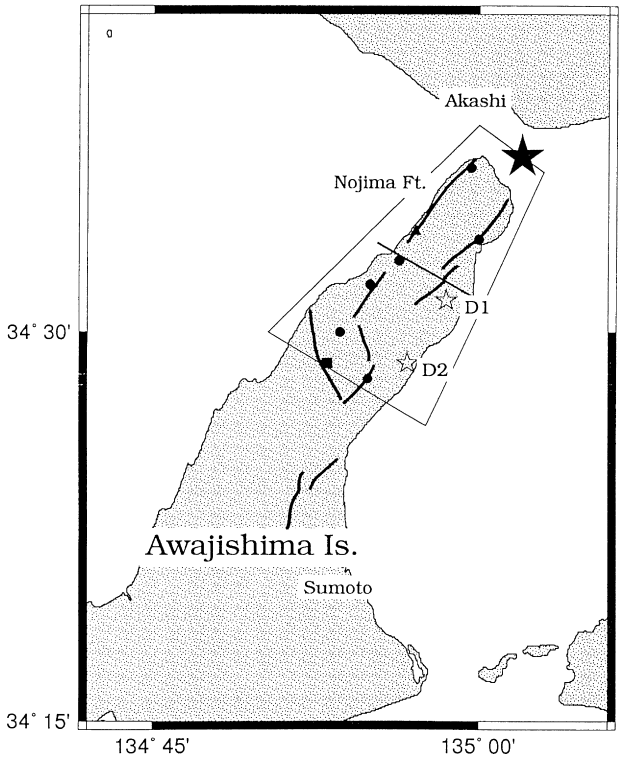

Fig. 1. Index map of the studied area. Most of the data (except for several water chemistry data) were obtained from inside the trapezoid. Filled star indicates the epicenter of the Kobe Earthquake, open stars the location of discharged water where the change of chemical composition was reported by Sato et al. (1995), filled square the location of a 1200 m deep well, dots the locations where Sato and Takahashi (1996) measured the relative discharge, a triangle the location where Oshima et al. (1996) measured the discharge rate, lines the location of active faults, and a straight line the location of the modeled cross section. See Fig. 2 for the schematic figure of the western half of the modeled cross-section.

Takamura and Kono, 1996), and it continued for more than 10 months. Observation (1) might be explained by the poroelastic response of the aquifer because the Island is situated in the compressional region of the co-seismic strain field (King et al., 1995). Observations (2)–(4) are very similar with that reported after the Loma Prieta Earthquake (Rojstaczer and Wolf, 1992; Rojstaczer et al., 1995), and may be explained by the enhancement of the permeability due to the earthquake. The following discussion will be concentrated on a simple model to explain the latter observations because poroelastic deformation has contributed

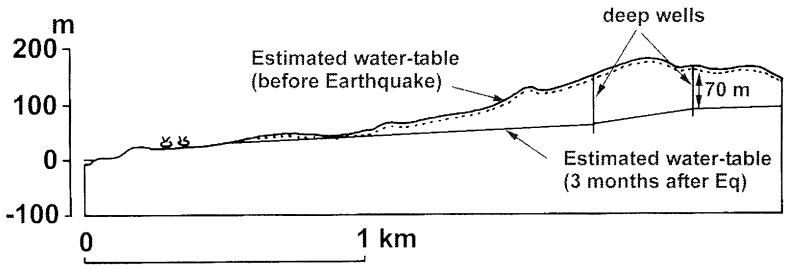

Fig. 2. Schematic cross-section showing the possible water-table drop at the northern part of the Awajishima Island. The water table at the western deep well before the Earthquake was not measured. There exist two discharge points. Modified after GRG (1996).

Table 1
Water-table fluctuations of shallow wells in the central part of the island (data after Oshima et al., 1996)

Well no.	Water table above well bottom (m)		Depth to well bottom (m)
	Before EQ	113 days after EQ[a]	
1	1.92	0.43	3.48
2	1.83	0.27	3.55
3	3.25	0.79	7.40
4	3.06	–	3.98
5	3.41	0.63	7.01
6	1.76	–	3.46
7	2.65	–	2.85
8	1.91	0.10	4.97
10	6.59	–	4.62
11	21.35	13.75	21.35
12	9.30	–	10.79
14	1.00	–	1.18
16	2.63	–	4.86
17	1.80	1.12	2.47
18	3.16	–	5.43
19	1.00	0.27	8.48

[a] Dashes indicate that no water existed in the well.

a minor amount of water discharge compared with that caused by permeability increase as will be discussed later.

2. Hydrological changes in the northern part of the Awajishima Island

Awajishima Island is situated very close to the epicenter (Fig. 1). Active faults run parallel and along the coastal lines (about 100–400 m away from the coast in the case of the Nojima Fault) of the northern part of the Island, and the Nojima Fault was ruptured by the Earthquake (Fig. 1). The central part of the Island consists mainly of weathered granite and

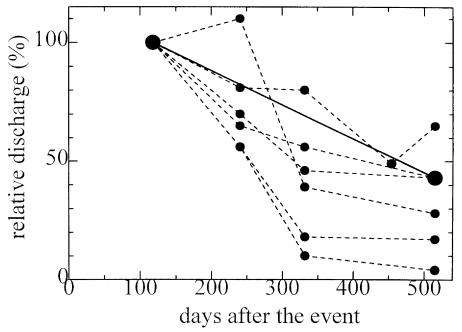

Fig. 3. Change of relative discharge (normalized by that in May 1995) as a function of time. Small dots and dotted lines indicate each measurement and large dots and a line indicate the overall change between May 1995 and June 1996. Data after Sato and Takahashi (1996).

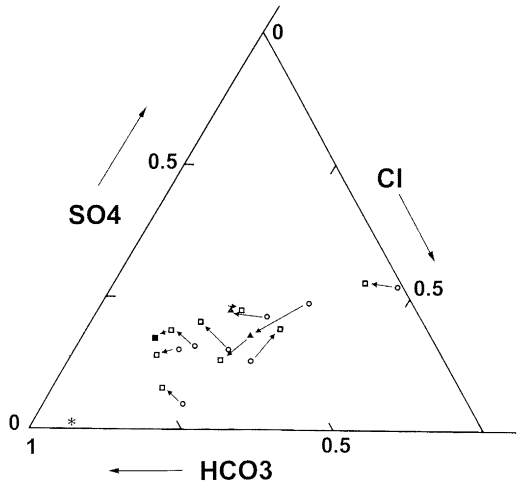

Fig. 4. Change of water chemistry (anions) due to the Earthquake. ○ Aug., 1994 (Hake & Nishimura, 1994), ▲ Jan., Feb., 1995 (Sato et al., 1995), □ Mar., 1995 (Takamura & Kono, 1996), ■ Oct., 1995, ∗ 1205 m well (Oct., 1995).

a thin cover of Neogene marine sediments. The elevation of the central part is more or less constant at around 200 m above sea level (the highest point is 360 m at the southernmost part in the studied area).

The water table in the central part of the Island before the Earthquake was close to the topographic surface and dropped to more than 70 m within 90 days after the Earthquake (GRG, 1996; Kumai, personal communication) (Fig. 2). The regional water-table distribution at 90 days after the Earthquake was estimated from two deep wells and discharge points (GRG, 1996; Kumai, personal communication). Considering the spatial distribution of the wells and discharge points, this estimation (Fig. 2) is reasonable. Shallow wells in the central part also dropped (Table 1) even though some of them still show the existence of water, which suggests the existence of local perched water systems. This water-table drop is significant compared with the possible magnitude of natural fluctuations. People have used shallow wells (less than 10 m in depth) (Table 1) for daily use, suggesting that the seasonal water-table fluctuation is smaller than 10 m. The 70 m drop of the water table cannot be explained by the annual fluctuation of recharge. Rainfall is heaviest in the summer season and is about four times larger than that in the winter season. The Earthquake happened on 17 January and the water table did not return after the summer season; instead it continued to drop except for two wells out of the 16 measured shallow wells (Oshima et al., 1996). The annual rainfall is about 1400 mm, and assuming that one-third of the annual rainfall is the recharge rate, it is necessary to consider more than 1 year of no rainfall for the water table to drop 70 m (assuming 1% porosity). Thus, it is reasonable to assume that natural fluctuations are smaller than the observed water-table drop, and the water-table drop can be attributed to the Earthquake-related phenomenon.

Sato and Takahashi (1996) reported the volumetric change of discharge at six locations between May 1995 and June 1996 (Fig. 1). The overall discharge in June 1996 was 43% of that in May 1995 (Fig. 3). Although they did not measure the entire volume of discharge over the Island, their locations are all situated at the major discharge points and also cover the studied area; thus, it can be assumed that the ratio of their measurements represents the ratio of the whole volume of discharge. Oshima et al. (1996) measured stream flow of four locations, located about 250 m from the coast, whose catchment areas extend about 500–600 m along the coast (Fig. 1). They measured an overall discharge of 1.75 m^3/min 290 days after the Earthquake. This value is about 1.3–1.6 times larger than the steady state value (integrated over a 500–600 m distance) obtained from the model which is described later, in the case where one-third of the annual rainfall is assumed to be the recharge rate.

The increase of discharge also is significant compared with the annual fluctuations. Sato and Takahashi (1995) reported that the water level of one of the ponds, which is located where Oshima et al. (1996) measured discharge, increased very rapidly just after the Earthquake even though no water existed there before the Earthquake. Considering that the dam was artificially broken within a day after the Earthquake to prevent it from overflowing, the increase of discharge must have been significantly larger than the annual fluctuations.

The chemical composition of discharged water resulted in an increase in bicarbonate after the Earthquake (Fig. 4). The change of chemical composition can be explained either by the mixing of discharged water at steady state and the deeper water represented by the 1205 m well; or by the discharge of water that had been side-tracked into dead-end pores and/or slow pathways through relatively less permeable rocks due to the possible earthquake-induced micro-fracturing, or some other reasons.

3. Construction of a model to explain the hydrological changes

GRG (1996) tried to estimate the increase in the permeability of the aquifer and reported that permeability increased 3.6 times after the Earthquake. However, as they did not show the model and assumptions used to obtain the value, it is difficult to evaluate their result. Rojstaczer et al. (1995) used a simple diffusion model to explain the phenomenon following the 1989 Loma Prieta Earthquake. They adopted a confined aquifer model and discussed the water-table drop of the mountainous region.

Here, the Dupuit–Ghyben–Herzberg (D–G–H) model (Bear, 1972; Fetter, 1972; Vacher, 1988; Vacher and Wallis, 1992) was applied to the unconfined fluid

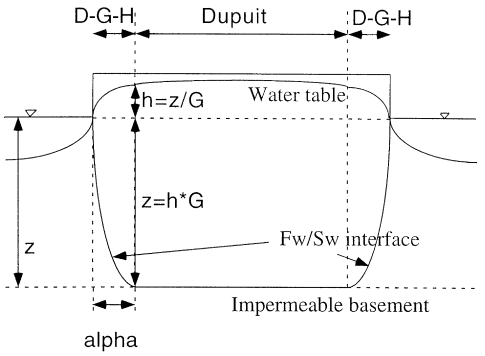

Fig. 5. A schematic figure of the model used in this study. D–G–H and Dupuit indicate the region where the Dupuit–Ghyben–Herzberg model and the simple Dupuit model are applied, respectively. See text for details.

flow in the Island. An infinite-strip island model can be applied due to the fact that the width of the northern part of the Island is around 5 km and more or less constant (Fig. 1). The D–G–H model results from combining (a) the Dupuit approximation of horizontal flow and (b) the Ghyben–Herzberg principle of proportionality between water-table elevation and depth to interface with (c) Darcy's law. The Dupuit approximation is violated near the coast where the thickness of the freshwater region narrows. However, this treatment might be acceptable because the relative change in discharge is used to estimate the relative change in the order of magnitude of the hydraulic properties by the earthquake. Although this earthquake may cause an increase in the vertical flow along faults, Ishimaru (1997) showed that the increase of vertical permeability along faults alone could not explain any water-table drop in the central part of the Island, suggesting that the increase of horizontal permeability can be a possible reason for the observed water-table drop.

The resulting D–G–H version of Darcy's law is combined with the continuity equation to give a governing differential equation (Vacher, 1988). However, it is not appropriate to directly apply the model to the Island because the depth of the freshwater–saltwater interface at the central part before the Earthquake is calculated to be 6.6 km, assuming that the water table is 165 m above sea level. This value is unrealistic considering the 5-km width of the Island. Instead, it is assumed that there is an impermeable basement below a specified depth and the fluid flow in the Island is governed by the combination of the D–G–H model (where the water table is below z/G) and the simple Dupuit model (where the water table is above z/G) (Fig. 5), and the effect of the position of the impermeable basement is examined in this analysis. Here z and G ($= \rho_w/(\rho_s - \rho_w)$) represent the depth of the basement from sea level and the Ghyben–Herzberg constant, respectively, and ρ_w is the density of freshwater and ρ_s is that of saltwater. Assuming that the porosity of the unweathered granite at depth is very small compared with the specific yield of the highly weathered surficial granite, the governing equations for unconfined groundwater flow in the Island becomes

$$K(1+G)\frac{\partial}{\partial x}\left(h\frac{\partial h}{\partial x}\right) + w = S_y\frac{\partial h}{\partial t} \quad (1)$$

for the D–G–H region of the model, and

$$K\frac{\partial}{\partial x}\left((h+z)\frac{\partial h}{\partial x}\right) + w = S_y\frac{\partial h}{\partial t} \quad (2)$$

for the simple Dupuit region of the model, where K is the hydraulic conductivity, h the height of the water table, w the recharge rate and S_y the specific yield. Because the boundary between the D–G–H and the simple Dupuit models moves with the change of water-table height, this combined model tracks the boundary (the length 'alpha' in Fig. 5) and maintains conservation of mass during the transient calculations. The mass conservation is held at the boundary between the models because $z = h \times G$ at the boundary (Fig. 5), and substituting this relationship into Eq. (2) shows that the same flux is obtained through the boundary from both Eqs. (1) and (2).

A numerical code has been developed based on the finite-difference approximation. The validity of the code was checked by comparing (1) the numerical and analytical solutions of the Boussinesq problem (Polubarinova-Kochina, 1962; Bear, 1972) for the simple Dupuit case and (2) the steady state results of both numerical and analytical solutions for the combined case.

4. Results of numerical calculation and discussion

The observed quantitative data have been used to

constrain the model. These are: (1) the water table at the central part of the Island dropped from 165 m above sea level to 95 m within 90 days after the Earthquake (GRG, 1996; H. Kumai, 1998 personal communication) (Fig. 2); (2) the overall discharge in June 1996 was 43% of that in May 1995 (Fig. 3); (3) the depth to the impermeable basement is greater than 1205 m. This constraint comes from the chemical composition of the 1205 m well water, which does not show saltwater features (Na^+ of 5.36 meq/l and Cl^- of 0.36 meq/l).

The initial condition is set as the steady state solution in which the water table at the center of the Island is 165 m above sea level, and is calculated using either the D–G–H model or the simple Dupuit model according to positions. The lower boundary is set as impermeable at the freshwater–saltwater interface for the D–G–H region and at the depth of the impermeable basement for the simple Dupuit region (Fig. 5). The condition for the lateral boundaries are set as 0 m height of the water table at the coastal lines. Recharge is assumed to be constant and is assumed to be either half, one-third, or one-fifth of annual rainfall.

Using the above mentioned model and boundary conditions, the optimal sets of the change of hydraulic conductivity due to the Earthquake and the specific yield were estimated. Fig. 6 shows how the calculated results change by changing these parameters. In this figure, solid contours show the absolute difference between the calculated and measured discharge ratio

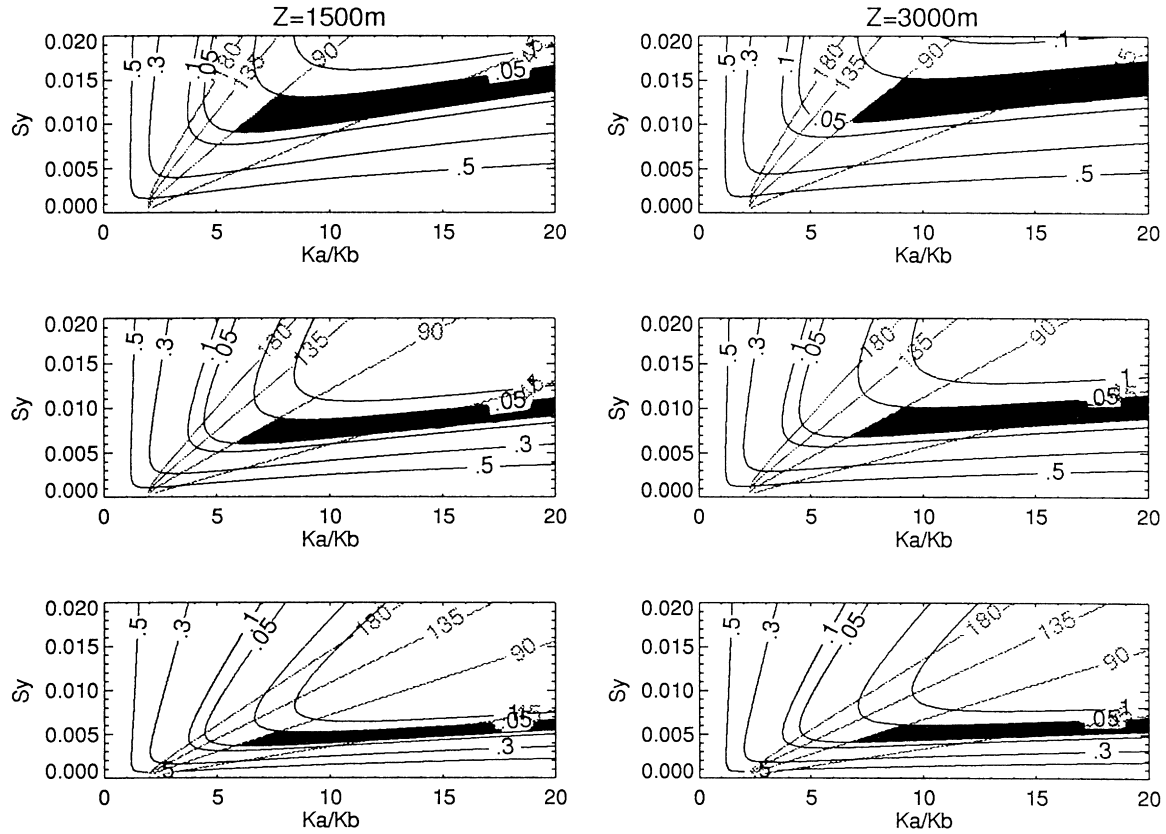

Fig. 6. Contour maps explaining how calculated results change due to changing parameters. Horizontal axis is the ratio between the hydraulic conductivity after (K_a) and before (K_b) the Earthquake, and the vertical axis the specific yield. Recharge is assumed to be half of the annual rainfall for the upper, one-third for the middle, and one-fifth for the bottom figures. Lines indicate the absolute difference between the calculated and measured discharge ratio and dotted line the date when the water table at the central part becomes below 95 m. The filled area is the region where the model is evaluated to be optimal.

between May 1995 and June 1996 and dotted contours indicate the date when the water table at the central part falls below 95 m. From constraint (1), the region above the 90 day contour is considered not to be optimal. Similarly, the region outside of the 0.05 solid contour is considered not to be optimal. Thus, the filled area is the region where the model is evaluated to be optimal.

It is found that the optimal specific yield is between 0.3 and 1.7% depending on the recharge rate but independent of the assumed depth to the impermeable basement (Fig. 6). This result is noteworthy because the estimates of specific yield are usually not so well constrained. The hydraulic conductivity is estimated to increase at least five times after the Earthquake (Fig. 6). The increase of hydraulic conductivity should be interpreted as the geometric average of the increase of the conductivities in the fault zone and the surrounding rocks. The increase of hydraulic conductivity in the fault zone might be larger than that of the surroundings. However, the thickness of the fault zone is very narrow compared with the thickness of the surrounding rocks considering the horizontal model used in this analysis, and it was not practical to explicitly account for faults as different hydraulic conductivity zones due to the scarcity of data sets. Thus, it was decided to estimate the geometric average of the change of hydraulic conductivity in this analysis.

Fig. 7a shows examples of the calculated change of discharge rate normalized by that at steady state as a function of time using the optimal sets of parameters. This result can be used to estimate the significance of poroelastic contribution to the discharge. Assuming a co-seismic volumetric strain of 10^{-5}, a Biot–Willis coefficient of 0.85 (Berryman, 1992), and a deformation depth of 10 km, which are all very large estimates, the total discharge changes 425 m^3 in a 1 m slice of the Island. This value is about 65 times larger than that of the assumed daily discharge at steady state condition (assuming one-third of rainfall as recharge). Even though this value is large, the increase of discharge due to the increase of hydraulic conductivity is an order of magnitude larger (integrate Fig. 7a); thus, the poroelastic contribution is considered to be very small.

It is obvious that the increase of the hydraulic conductivity is proportional to the increase of discharge just after the earthquake, and that it is difficult to estimate the increase of conductivity using the discharge data 100 days after the earthquake, which is the case for this analysis (Fig. 3). This suggests that it is important to measure the change of discharge just after the earthquake to obtain a proper estimate of the change of hydraulic conductivity. Fig. 7b shows the calculated water-table change as a function of time. This result indicates that it is also difficult to obtain the increase of the conductivity from the measurements of the water-table drop at the central part of the Island.

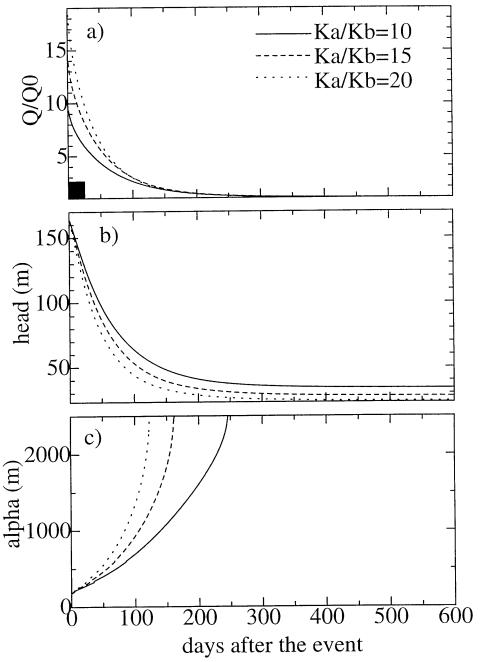

Fig. 7. Examples of calculated: (a) discharge rate normalized by that at steady state condition; (b) water table at the center of the Island; and (c) location of freshwater–saltwater boundary at the depth of impermeable basement, from the optimal sets of hydraulic properties (in the case where $z = 1500$ m, recharge is one-third of rainfall). Solid box in (a) indicates the equivalent volume of poroelastic contribution.

Fig. 7c shows the amount of saltwater invasion due to the drop of water table (see Fig. 5 for the definition of vertical axis). This result suggests that saltwater has intruded into the aquifer in accordance with the Ghyben–Herzberg principle. The saltwater intrusion could be the cause of the mixing of shallower and deeper water and could be the reason why the

chemical composition has changed (Fig. 4). Note that this analysis does not necessarily support the interpretation because the flow direction is assumed to be horizontal and because the porosity of deeper granite is very small, neglecting the contribution of deeper groundwater to the calculated discharge. However, once the hydraulic conductivity is increased and approaches a new steady state condition, it is suggested that the shape of the freshwater zone narrows and deeper groundwater could discharge at around the coastal zone. More sophisticated modeling is necessary to fully take the contribution of the migration of deeper water into consideration.

5. Conclusions

Several hydrologic changes were observed in Awajishima Island caused by the Kobe Earthquake. A combined Dupuit–Ghyben–Herzberg and simple Dupuit model was constructed to test the ability to explain these phenomena. This model can explain the most of the phenomena consistently, and the following conclusions are obtained:

1. Increase of horizontal hydraulic conductivity by the Earthquake may be the main cause of hydrologic changes and the hydraulic conductivity is estimated to increase at least five-fold after the Earthquake.
2. It is necessary to measure the increase of discharge just after the earthquake to better constrain the increase of the hydraulic conductivity.
3. Contribution to discharge by co-seismic volumetric strain is calculated to be minor.
4. The specific yield of the unconfined aquifer is estimated to be 0.3–1.7% depending on the recharge rate but independent of the assumed depth to the impermeable basement.
5. Change of chemical composition of discharged water could be caused by the movement of deeper water due to the intrusion of saltwater into the aquifer, however, more sophisticated analysis is necessary to prove this hypothesis.

Acknowledgements

H.F. Wang, D.J. Hart and T.L. Masterlark gave me helpful comments and suggestions for the analysis. H. Kumai, the chief scientist of GRG, kindly provided me information on the date of their measurements. This manuscript benefited greatly from the careful and constructive reviews by Barbara Bekins, Chi-Yu King, and an anonymous referee. The author gratefully acknowledges the Murata Overseas Scholarship Foundation for providing financial support to visit the University of Wisconsin-Madison.

References

Bear, J., 1972. Dynamics of Fluids in Porous Media, Elsevier, New York 764 pp.

Berryman, J.G., 1992. Effective stress for transport properties of inhomogeneous porous rock. Journal of Geophysical Research 97, 17 409–17 424.

Fetter Jr., C.W., 1972. Position of the saline water interface beneath oceanic islands. Water Resources Research 8, 1307–1315.

Groundwater Research Group, Osaka city University Investigation Team for the Hanshin-Awaji Great Earthquake Disaster (GRG), 1996. Influence by the Hyogoken-Nanbu Earthquake to the groundwater including hotspring water. In: Shibasaki, T., Uemura, T., Yoshimura, T. (Eds.). Great Earthquakes, Geologists' Roles in Time of Disaster, Tokai University Press, pp. 133–147.

Hake, Y., Nishimura, R., 1994. Visit to valuable water springs (27). Valuable water springs in Awaji island. Journal of Groundwater Hydrology 36, 487–492.

Ishimaru, T., 1997. Study for long-term stability of geological environment—seismic effect on hydrogeological environment. PNC Technical Review (102), 39–46.

King, C.-Y., Koizumi, N., Kitagawa, Y., 1995. Hydrogeochemical anomalies and the 1995 Kobe Earthquake. Science 269, 38.

Muir-Wood, R., King, G.C.P., 1993. Hydrological signature of earthquake strain. Journal of Geophysical Research 98, 22 035–22 068.

Osada, M., Tokunaga, T., Ishibashi, H., Kayaki, T., 1997. Groundwater fluctuations in the northern part of Awaji Island after Hyogoken-Nanbu Earthquake. In: Proceedings of the 1997 Annual Meeting of the Japan Society of Engineering Geology, pp. 237–240.

Oshima, H., Tokunaga, T., Miyajima, K., Tanaka, K., Ishibashi, H., 1996. Groundwater fluctuations caused by the earthquake. Journal of the Japan Society of Engineering Geology 37, 351–358.

Polubarinova-Kochina, P.Ya, 1962. Theory of Ground Water Movement, Princeton University Press, Princeton 613 pp.

Rojstaczer, S., Wolf, S., 1992. Permeability changes associated with large earthquakes: an example from Loma Prieta, California. Geology 20, 211–214.

Rojstaczer, S., Wolf, S., Michel, R., 1995. Permeability enhancement in the shallow crust as a cause of earthquake induced hydrological changes. Nature 373, 237–239.

Sato, T., Takahashi, M., Matsumoto, N., Tsukuda, E., 1995.

Anomalous ground water discharge after the 1995 Kobe (Hyogo-ken-nanbu) earthquake in the Awaji island, Japan. Chishitsu News (496), 61–66.

Sato, T., Takahashi, M., 1996. Anomalous ground water discharge after the Kobe (Hyogo-ken-nanbu) earthquake in the Awaji Island, Japan (part 2): change of the discharge rate. Chishitsu News (506), 24–28.

Sibson, R.H., 1981. Fluid flow accompanying faulting: field evidence and models. In: Simpson, D.W., Richards, P.G. (Eds.). Earthquake Prediction, American Geophysical Maurice Ewing Series, Vol. 4, pp. 593–603.

Takamura, H., Kono, T., 1996. Trend of spring water and groundwater in the Awaji Island after the 1995 Hyogo-nanbu earthquake. Journal of Groundwater Hydrology 38, 331–338.

Vacher, H.L., 1988. Dupuit–Ghyben–Herzberg analysis of strip-island lenses. Geological Society of America Bulletin 100, 580–591.

Vacher, H.L., Wallis, T.N., 1992. Comparative hydrogelogy of fresh-water lenses of Bermuda and Great Exuma Island, Bahamas. Ground Water 30, 15–20.